Polarization selective ultra-broadband wavelength conversion in silicon nitride waveguide

Arman Ayan[1*], Florent Mazeas[1], Junqiu Liu[2], Tobias Kippenberg[2], Camille-Sophie Brès[1]

[1] École Polytechnique Fédérale de Lausanne, Photonic Systems Laboratory (PHOSL), STI-IEL, Station 11, CH-1015 Lausanne, Switzerland

[2] École Polytechnique Fédérale de Lausanne, Laboratory of Photonics and Quantum Measurements (LPQM), SB-IPHYS, Station 3, CH-1015 Lausanne, Switzerland

arman.ayan@epfl.ch

Abstract We report broadband continuous-wave frequency conversion from the O-band (1.33 µm) to the short-wave infrared (2.6 µm) in a 50 cm long low-loss Si_3N_4 waveguide, leveraging polarization selective far-detuned phase matching.

Introduction

Nonlinear integrated photonics has drawn a great deal of attention[1]. Strong nonlinear interactions can be obtained at the device level as a result of high optical confinement and the availability of highly nonlinear materials. Stoichiometric silicon nitride (Si_3N_4) is a promising candidate for providing CMOS compatibility, low linear loss, relatively high nonlinear coefficient, large transparency window from the visible to the mid-infrared and high bandgap all together. Moreover, Si_3N_4 can provide intriguing dispersion characteristics, which can be employed to obtain coherent mid-infrared sources. These sources can pave the way for on-chip sensing and spectroscopy[2].

Broadband and efficient continuous wave (CW) four-wave mixing (FWM) remains a particularly challenging task. When pump power is limited, as often the case in CW regime, the trade-off between bandwidth and conversion efficiency (CE) is hard to overcome[3]-[5]. Recent progress in the fabrication now reaches linear losses in the dB/m in large cross-section Si_3N_4 waveguide, allowing for meter-long waveguides and possible increase in FWM CEs[6]. However, dispersion engineering becomes critical as to avoid limiting the bandwidth of operation.

In this work, we demonstrate ultra-broadband CW FWM in a L = 50 cm long Si_3N_4 waveguide, leveraging distant conversion through higher-order dispersion terms. Our design can generate idlers from the O-band (1.3 µm) to 2.5 µm by leveraging polarization-distinct phase-matching conditions. Waveguide engineering results in a zero-dispersion wavelength (ZDW) in the telecom band for TM polarization, while for TE polarization a ZDW appears in the thulium (2 µm) spectral band. Higher-order dispersion allows for the appearance of far detuned phase-matched wavelengths on the blue side for TM and on the red side for TE, simply by mixing the telecom and 2 µm band.

Waveguide and experimental setup

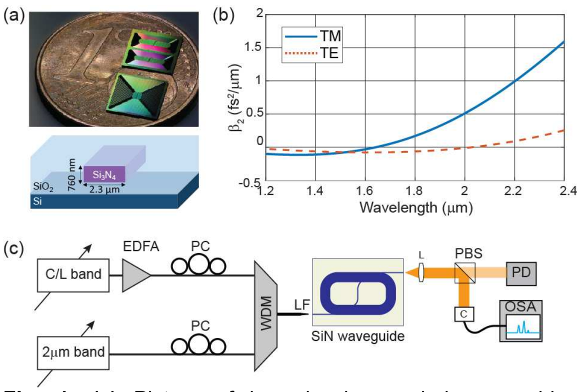

Fig. 1: (a) Picture of long low-loss spiral waveguides fabricated with the optimized Damascene process and cross-section of the waveguide used in this work. **(b)** Simulated dispersion curves for TE and TM modes for the 0.755 x 2.3 µm^2 waveguide.; **(c)** experimental setup. EDFA: erbium doped fiber amplifier, TDFA: thulium doped fiber amplifier, PC: polarization controller, LF: lens fiber, WDM: wavelength division multiplexer, PBS: polarization beam splitter, PD: photodiode, OSA: optical spectrum analyzer.

The Si_3N_4 waveguide used in this work has dimensions approximately of 2.3 µm width, 760 nm height, is fully cladded in SiO_2 and is tapered from both ends. The length of the waveguide is 50 cm, folded in meanders (Fig. 1a). The waveguides are fabricated with an optimized photonic Damascene process[7] resulting in ultra-low losses estimated for our chip at less than 4 dB/m. The dispersion of the waveguide is simulated by a finite-element method on COMSOL and is plotted in Fig. 1b for fundamental TE and TM. The dispersion for the TE mode is low and flat over the entire telecom band and a ZDW appears near 2.05 µm, within the thulium amplification band. For the TM mode, we observe a ZDW near 1.65 µm.

The experimental setup is shown in Fig. 1c. We use a tunable C/L-band source amplified with an EDFA and a homemade thulium-doped fiber laser (TDFL) tunable between 1820 to 2000 nm as input sources. For TE polarization, the TDFL serves as the pump while the C/L-band source serves as the signal. The opposite configuration is used for TM polarization. The polarization of the pump and signal is carefully controlled at the input of the waveguide and is monitored at the output of the waveguide by the use of a polarization beam splitter and a photodiode, to ensure that the state of polarization is constant during the wavelength sweeps. The pump and signal are combined by a wavelength division multiplexer and coupled into the waveguide by a lensed fiber. The light is collected at the output with an objective and a collimator. We estimate that the coupled pump power is 20 dBm for TE polarization (telecom band pump) and 17 dBm for TM polarization (thulium band pump). The CE of the FWM process is estimated based on the measured spectra using an optical spectrum analyzer operating between 1.5 and 3.4 μm (Yokogawa AQ6376) and between 1.2 and 2.4 μm (Yokogawa AQ6375B) for TE and TM, respectively.

Results

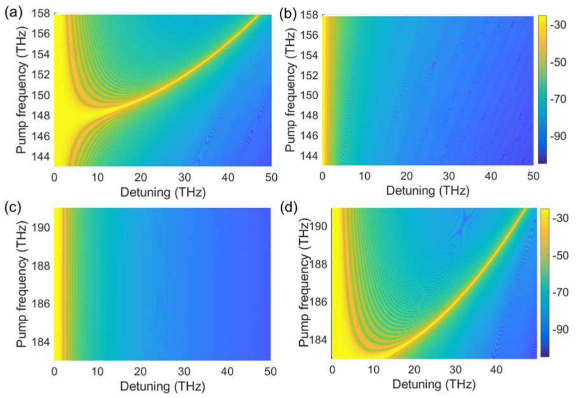

Fig. 2. Theoretical contour graph of CE (dB) for **(a)** TE polarization and **(b)** TM polarization for pumping in the thulium band with 100 mW pump power; **(c)** TE polarization and **(d)** TM polarization for pumping in the telecom band with 50 mW pump power

While one can expect efficient FWM near the ZDW of 1.7 μm/2.1 μm for TM/TE pumping, higher-order dispersion terms can play a significant role and can lead to far-detuned region of parametric conversion. In Fig. 2, we plot the map of CE which depends on the propagation constant mismatch $\Delta\beta L = \left(2\beta_p - \beta_s - \beta_i\right)L$, with $\beta_{p,s,i}$ the propagation constant at the pump, signal and idler, respectively, as a function of pump frequency and signal/idler detuning.

For TE polarization, the simulation results indicate that we should observe distant FWM for pump frequencies 149 THz and 156 THz for TE polarization (corresponding to 1921 – 2012 nm). The expected detuning is around 35 THz, compatible with a telecom band signal (Fig. 2a). The simulations also show that our relatively large cross-section waveguide can support mode propagation until 113 THz (~ 2650 nm) compatible with such detuning. No distant conversion can be obtained when the pump is located in the C/L band (Fig. 2b). For TM polarization, the simulation indicates that distant phase-matching can be satisfied for a pump in the L-band (185 – 192 THz, or 1561 – 1620 nm). Once again, the expected detuning is around 30 THz, allowing for the generation phase-matched idler in the O/E-band from 2 μm signals (Fig. 2d). However, no distant conversion occurs in TE when pumping in the thulium band (Fig. 2c).

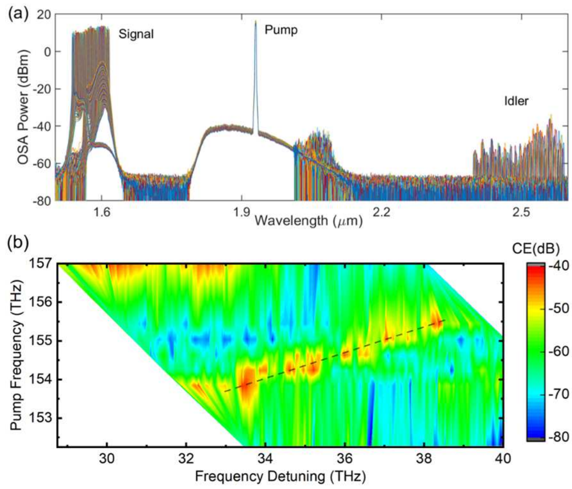

Fig. 3: Experimental results for TE polarization. **(a)** Spectra from 1.5 μm to 2.6 μm for a 1930 nm pump and the signal swept from 1538 nm to 1615 nm. **(b)** Measured CE values for pump wavelengths of 1910, 1930, 1935, 1940, 1945, 1950, and 1970 nm, and signal swept from 1538 to 1615 presented in contour graph vs pump frequencies and frequency detuning values.

The measured spectra for TE polarization and a 1930 nm of pump are shown in Fig. 3a. The idler can be generated between 2.4 μm to 2.6 μm as the signal wavelength is swept from 1615 nm to 1538 nm. The idler reaches the highest power around 2550 nm, which is in agreement with the simulation results. The same experiment was repeated for 1910, 1935, 1940, 1945, 1950, and 1970 nm pump wavelengths. In all cases, the coupled pump power is approximately 20 dBm, while the signal is between 10 and 15 dBm. All the experimentally measured values of CE are plotted in Fig. 3b. We can see that the frequency detuning at which the phase matching occurs shifts from 33 THz to 39 THz as the pump frequency moves from 153.8 THz to 155.4 THz (indicated by the dashed line), in good agreement with the trend depicted in Fig. 2a. This corresponds to an efficient conversion between 2450 to 2550 nm by tuning the pump wavelength between 1910 and 1970 nm. We observe that around 2660 nm, there is a significant drop in the CE, in agreement with the simulated cut-off wavelength of the waveguide. The maximum CE is measured at around -40 dB for the 100 mW CW pump. The nonlinear coefficient γ is estimated at around 0.3 $W^{-1}m^{-1}$, in agreement with the simulations predicting 0.5 $W^{-1}m^{-1}$.

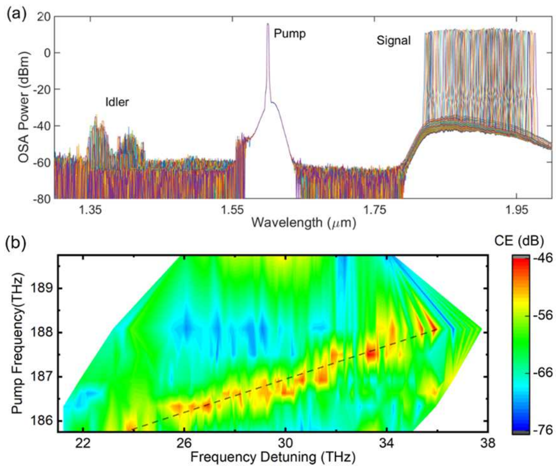

Fig. 4: Experimental results for TM polarization. (a) Spectra from 1.3 μm to 2.0 μm for the pump wavelength of 1600 nm, for the signal wavelengths swept from 1821 nm to 1975 nm. (b) Measured CE values for pump wavelengths of 1615, 1610, 1607.5, 1605, 1600, 1595, and 1580 nm, and signal swept from 1821 to 1990 nm presented in contour graph vs pump frequencies and frequency detuning values.

The same experiment is repeated after the polarizations are set to TM. The idler is now being projected to shorter wavelengths. The experimental spectra for 1600 nm pump are shown in Fig. 4a. The idler wavelengths shift from 1430 nm to 1330 nm as the signal moves from 1820 nm to 1975 nm. The maximum idler power is obtained around 1360 nm as expected according to the simulations. Once again, the experimentally measured CE values for pump wavelengths of 1615, 1610, 1607.5, 1605, 1600, 1595, and 1580 nm are presented in Fig 4b. The pump power is about 17dBm and the signal around 10 dBm. The frequency detuning at which phase matching is satisfied moves from 24 THz to 35 THz when the pump frequency moves from 185.7 to 188 THz (indicated by the dashed line), which is more significant than that of TE polarization, and still in agreement with the trend of Fig. 2b. This corresponds to a peak of the CE moving from 1420 nm to 1340 nm. The conversion is less efficient for TM polarization due to higher coupling loss compared to the TE polarization, reaching -46 dB for the 50 mW pump.

The measured distant phase matched spectra are not as narrow or smooth (multiple peaks are observed) as expected from theory and simulations. As distant conversion is sensitive to dispersion, small fluctuations along the waveguide, even minute, can lead to such behavior, as typically observed in optical fibers. Another consequence is the lower measured CE compared to theoretically predicted. The experimental characterization of waveguides of different lengths could lead to some more information related to this broadening behavior. Given the linear loss of recently fabricated waveguides (close to 1 dB/m), lengths up to 2 m while maintaining such dispersion engineering are now possible.

Conclusions

We have shown far-detuned continuous-wave frequency conversion between telecom and a 2 μm waves. By controlling the polarization of the waves, idlers can either be generated on the short wavelength side down to the O-band (for TM) or up towards the middle-infrared (for TE). Efficiencies of -40 dB for 100 mW of pump are obtained in TE, while -46 dB is measured for 50 mW of pump in TM. Owing to dispersion properties and the low loss features of our Si_3N_4 waveguides, the CE could be further increased by using longer waveguides. Contrary to other low-loss waveguides[4], further dispersion engineering is also possible, for example, to shift the TM ZDW in the telecom band and the TE ZDW closer to 2 um as to enable continuous broadband operation since pumping directly at the ZDW would be possible with standard fiber laser sources as used here.

Acknowledgments

The work is in part supported by SNSF BRIDGE (Project No: 182414).

References

[1] J. Leuthold, C. Koos, and W. Freude, “Nonlinear silicon photonics,” *Nature Photonics*, vol. 4, no. 8, pp. 535–544, 2010.

[2] A. Subramanian et al., “Silicon and silicon nitride photonic circuits for spectroscopic sensing on-a-chip [Invited],” *Photonics Research*, vol. 3, no. 5, 2015.

[3] M. Pu et al., “Ultra-Efficient and Broadband Nonlinear AlGaAs-on-Insulator Chip for Low-Power Optical Signal Processing,” *Laser & Photonics Reviews*, vol. 12, no. 12, p. 1800111, 2018.

[4] C. J. Krückel et al., “Continuous wave-pumped wavelength conversion in low-loss silicon nitride waveguides,” *Optics Letters,* vol. 40, no. 6, p. 875, 2015.

[5] C. J. Krückel, “Linear and nonlinear characterization of low-stress high-confinement silicon-rich nitride waveguides,” *Optics Express*, vol. 23, no. 20, p. 25827, 2015.

[6] F. Mazeas et al., “Low-loss SiN waveguides for efficient and broadly tunable nonlinear frequency conversion,” *OSA Advanced Photonics Congress (AP)*

2020 (IPR, NP, NOMA, Networks, PVLED, PSC, SPPCom, SOF), 2020.

[7] J. Liu et al., "High-yield, wafer-scale fabrication of ultralow-loss, dispersion-engineered silicon nitride photonic circuits," *Nature Communications*, vol. 12, no. 1, pp. 1-9, 2021